Mechanism of Protonation of $[Pt_3(\mu\text{-}PBu^t_2)_3(H)(CO)_2]$, Yielding the Hydride-Bridged $[Pt_3(\mu\text{-}PBu^t_2)_2(\mu\text{-}H)(PBu^t_2H)(CO)_2]OTf$ (Tf = CF_3SO_2), and the Spectroscopic and Theoretical Characterization of a Kinetic Intermediate

Alessandro Fortunelli,*,† Piero Leoni,*,‡ Lorella Marchetti,‡ Marco Pasquali,‡ Francesco Sbrana,‡ and Massimo Selmi†

Dipartimento di Chimica e Chimica Industriale dell' Università di Pisa, Via Risorgimento 35, and Istituto di Chimica Quantistica ed Energetica Molecolare (ICQEM) del CNR, Via V. Alfieri 1, I-56010 Ghezzano (Pisa), Italy

Received November 20, 2000

The reaction of the Pt(I)Pt(I)Pt(II) triangulo cluster $Pt_3(\mu\text{-}PBu^t_2)_3(H)(CO)_2$ (**1**) with TfOH (Tf = CF_3SO_2) affords the hydride-bridged cationic derivative $[Pt_3(\mu\text{-}PBu^t_2)_2(\mu\text{-}H)(PBu^t_2H)(CO)_2]OTf$ (**2**). With TfOD the reaction gives selectively $[Pt_3(\mu\text{-}PBu^t_2)_2(\mu\text{-}D)(PBu^t_2H)(CO)_2]OTf$ (**2-D**$_1$), implying that the proton is transferred to a metal center while a P−H bond is formed by the reductive coupling of one of the bridging phosphides and the terminal hydride ligand of the reagent. The reaction proceeds through the formation of a thermally unstable kinetic intermediate which was characterized at low temperatures, and was suggested to be the CO-hydrogen-bonded (or protonated) $[Pt_3(\mu\text{-}PBu^t_2)_3(H)(CO)_2]\cdot HOTf$ (**3**). An ab initio theoretical study predicts a hydrogen-bonded complex or a proton-transfer tight ion pair as a possible candidate for the structure of the kinetic intermediate.

Introduction

Platinum clusters with hydride ligands are important models of heterogeneous catalysts based on platinum surfaces.[1] However, although the chemistry of mono- and dinuclear platinum hydrides has been, and still is, extensively investigated,[2] relatively few tri- or polynuclear systems have been reported.[3−7a] Some tri- and tetranuclear hydride derivatives of platinum have been described by Puddephatt and co-workers[3] in their systematic approach to the chemistry of dppm-bridged triangulo clusters with a central $Pt_3(\mu\text{-dppm})_3$ core, and by Spencer and co-workers,[4] who described a series of clusters of general formula $[Pt_xH_y(PR_3)_x]^{m+}$ ($x = 3$, $y = 6$; $x = 4$, $y = 1, 2, 4, 7, 8$; $m = 0-2$). Other sporadic examples are $[Pt_3(\mu_3\text{-}H)(H)_2(dppe)_3]^+$,[5a] $[Pt_4(\mu\text{-}CO)_3(CO)(H)(PCy_3)_4]ReO_4$,[5b] and $[Pt_3(\mu_3\text{-}H)(\mu\text{-}CO)_3(PCy_3)_3]^+$,[5c] the latter obtained by protonation of one of the well-known triangulo derivatives $[Pt(\mu\text{-}CO)(PR_3)]_3$. To the best of our knowledge, until recently $[Pt_3(\mu\text{-}PPh_2)_2(\mu\text{-}H)(PPh_3)_3]^+$ was the unique phosphido-bridged derivative of this type,[6] and we reported a second example, the mixed-valence complex $[Pt_3(\mu\text{-}PBu^t_2)_3(CO)_2(H)]$ (**1**).[7a]

The mechanism of the reaction of **1** with TfOH, yielding the hydride-bridged $[Pt_3(\mu\text{-}PBu^t_2)_2(\mu\text{-}H)(CO)_2(PBu^t_2H)]OTf$ (**2**), and the nature of a kinetic intermediate observed at low temperatures are discussed herein.

Scheme 1

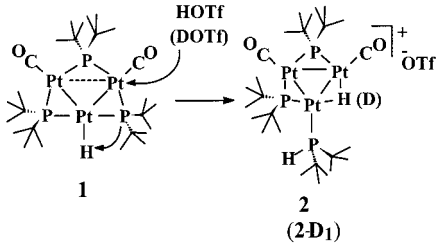

Results and Discussion

An orange dichloromethane solution of complex **1** quickly turned yellow after the addition of an equimolar amount of TfOH. After the solution was stirred for 2 h at room temperature, $[Pt_3(\mu\text{-}PBu^t_2)_2(\mu\text{-}H)(CO)_2(PBu^t_2H)]OTf$ (**2**) was isolated as a yellow microcrystalline solid (Scheme 1).

The IR spectrum of complex **2** shows absorptions at 2050, 2026 (ν_{CO}), 1272, 1147, 1032, and 637 (uncoordinated triflate) cm^{-1}.[8] The formation of a secondary phosphine during the protonation reaction can easily be argued by the $^{31}P\{^1H\}$ NMR spectrum of **2**, which shows two signals (394.1 and 348.0 ppm)

† ICQEM.
‡ Università di Pisa.

(1) Ramachandran, R.; Payne, N. C.; Puddephatt, R. J. *J. Chem. Soc., Chem. Commun.* **1989**, 128.
(2) Leoni, P.; Manetti, S.; Pasquali, M. *Inorg. Chem.* **1995**, *34*, 749−752 and references therein.
(3) (a) Hao, L.; Jobe, I. R.; Vittal, J. J.; Puddephatt, R. J. *Organometallics* **1995**, *14*, 2781. (b) Payne, N. C.; Ramachandran, R.; Schoettel, G.; Vittal, J. J.; Puddephatt, R. J. *Inorg. Chem.* **1991**, *30*, 4048. (c) Douglas, G.; Manojlovic-Muir, L.; Muir, K. W.; Jennings, M. C.; Lloyd, B. R.; Rashidi, M.; Puddephatt, R. J. *J. Chem. Soc., Chem. Commun.* **1988**, 149. (d) Rashidi, M.; Puddephatt, R. J. *Organometallics* **1988**, *7*, 1636. (e) Jennings, M. C.; Payne, N. C.; Puddephatt, R. J. *Inorg. Chem.* **1987**, *26*, 3776. (f) Jennings, M. C.; Payne, N. C.; Puddephatt, R. J. *J. Chem. Soc., Chem. Commun.* **1986**, 1809. (g) Rashidi, M.; Puddephatt, R. J. *J. Am. Chem. Soc.* **1986**, *108*, 7111. (h) Lloyd, B. R.; Puddephatt. R. J. *J. Am. Chem. Soc.* **1985**, *107*, 7785.
(4) (a) Goodfellow, R. J.; Hamon, E. M.; Howard, J. A. K.; Spencer, J. L.; Turner, D. G. *J. Chem. Soc., Chem. Commun.* **1984**, 1604. (b) Frost, P. W.; Howard, J. A. K.; Spencer, J. L.; Turner, D. G. *J. Chem. Soc., Chem. Commun.* **1981**, 1104.
(5) (a) Carmichael, D.; Hitchcock, P. B.; Nixon, J. F.; Pidcock, A. *J. Chem. Soc., Chem. Commun.* **1988**, 1554. (b) Hao, L.; Vittal, J. J.; Puddephatt, R. J.; Manojlovic-Muir, L.; Muir, K. W. *J. Chem. Soc., Chem. Commun.* **1995**, 2381. (c) Dahmen, K. H.; Imhof, D.; Venanzi, L. M. *Helv. Chim. Acta* **1994**, *77*, 1029.
(6) Bellon, P. L.; Ceriotti, A.; Demartin, F.; Longoni, G.; Heaton, B. T. *J. Chem. Soc., Dalton Trans.* **1982**, 1671.
(7) (a) Leoni, P.; Manetti, S.; Pasquali, M.; Albinati, A. *Inorg. Chem.* **1996**, *35*, 6045. (b) Leoni, P.; Pieri, G.; Pasquali, M. *J. Chem. Soc., Dalton Trans.* **1998**, 657.

10.1021/ic001309m CCC: $20.00
Published on Web 05/19/2001

Chart 1

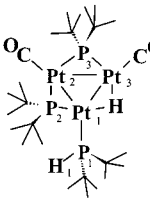

Isotopomer		%
A	Pt_1,Pt_2,Pt_3	29.0
B	$^{195}Pt_1,Pt_2,Pt_3$	14.8
C	$Pt_1,{}^{195}Pt_2,Pt_3$	14.8
D	$Pt_1,Pt_2,{}^{195}Pt_3$	14.8

for the unequivalent phosphides, and one [77.5 ppm, broad doublet ($^1J_{PH}$ = 366 Hz) in the corresponding proton-coupled spectrum] for the coordinated PBu^t_2H molecule. As suggested by the position of their P resonances,[2] each phosphide bridges two metal−metal-bonded platinum centers. The spectrum consists of the usual sum of subspectra arising from the various isotopomers of cation $\mathbf{2}^+$, with a different content of the NMR-active ^{195}Pt nucleus (I = $^1/_2$, NA = 33.8%); the numbering scheme and a table showing the composition of the most abundant isotopomers are shown in Chart 1.

The central resonances of each signal (isotopomer **A**) appear as doublets of doublets ($^2J_{P_1P_2}$ = 22.4 Hz, $^2J_{P_2P_3}$ = 195 Hz, and $^3J_{P_1P_3}$ = 8.4 Hz), suggesting that P_1 and P_2 are in pseudo-*cis* and P_2 and P_3 are in pseudo-*trans* mutual position. Each signal is flanked by two different sets of ^{195}Pt satellites (isotopomers **B**−**D**), yielding the values of $^1J_{P_1Pt_1}$ = 3590 Hz, $^2J_{P_1Pt_2}$ = 280 Hz, and $^2J_{P_1Pt_3}$ = 306 Hz (from the satellites of P_1), $^1J_{P_2Pt_1}$ = 2624 Hz, $^1J_{P_2Pt_2}$ = 1450 Hz, and $^2J_{P_2Pt_3} \cong$ 0 Hz (from the satellites of P_2), and $^1J_{P_3Pt_2}$ = 1729 Hz, $^1J_{P_3Pt_3}$ = 2100 Hz, and $^2J_{P_3Pt_1}$ = 47.5 Hz (from the satellites of P_3).

These assignments have been confirmed by the ^{195}Pt{^{1}H} NMR spectrum, which shows three signals centered at −3542.5 (Pt_3), −4335 (Pt_1), and −4831 (Pt_2) ppm. The stronger lines of these signals, respectively, appear as a dd (J_{PtP} = 306, 2100 Hz, isotopomer **D**), a ddd (J_{PtP} = 3590, 2624, 47.5 Hz, isotopomer **B**), and a ddd (J_{PtP} = 1729, 1450, 280 Hz, isotopomers **C**). These multiplets are flanked by weaker lines for the isotopomers with at least two ^{195}Pt nuclei, which provide the values of $^1J_{Pt_2Pt_3}$ = 3573 Hz, $^1J_{Pt_1Pt_3}$ = 3800 Hz, and $^1J_{Pt_1Pt_2}$ = 3672 Hz. In the corresponding proton-coupled spectrum the signals for Pt_3 and Pt_1 are further split by the large coupling to the bridging hydride, $^1J_{Pt_3H}$ = 888 Hz, $^1J_{Pt_1H}$ = 850 Hz.

The ^{1}H NMR spectrum exhibits the resonance for the bridging hydride at +6.2 ppm (dddd, coupled to three different P nuclei and to H_1, $^2J_{HP}$ = 14, 46, 61 Hz, $^3J_{HH}$ = 2.8 Hz). The signal is flanked by two different sets of satellites, giving the same values shown above for the couplings to Pt_3 and Pt_1. Although unusual for a metal hydride, the low-field position of δ_H has numerous precedents.[9] These examples generally concern d^0 or d^{10} systems; however, some di- or trinuclear (non-d^{10}) platinum hydrides are known to give positive values of δ_H[9e−g] (for example, $\delta_{\mu-H}$ = +4.16 ppm for $[Pt_3(\mu\text{-dppm})_3(\mu\text{-H})]^+$).[9e]

The P−H proton gives a double multiplet ($^1J_{PH}$ = 366 Hz) at 6.01 ppm, and the *tert*-butyl protons give three overlapped doublets (1.50−1.60 ppm).

Mechanism of the Proton-Transfer Reaction. As shown in Scheme 1, the reaction could occur through the protonation of a platinum center, accompanied by the formation of a P−H bond from one of the phosphides and the hydride ligand. Alternatively, the secondary phosphine could form by the direct protonation of a bridging phosphide, while the terminal hydride shifts to the bridging position. Actually, $[Pt_3(\mu\text{-}PBu^t_2)_2(\mu\text{-D})(PBu^t_2H)(CO)_2]$OTf (**2-D**$_1$) was selectively formed when complex **1** was reacted with TfOD (Scheme 1), which strongly supports the former mechanism.

The position of deuterium in **2-D**$_1$ was clearly indicated by its ^{1}H NMR spectrum, which shows all the resonances given by complex **2**, except the hydride signal at 6.2 ppm (a very weak signal here was attributed to a small amount of nondeuterated acid in the commercial sample of TfOD).

The ^{31}P{^{1}H} NMR spectrum was practically unchanged, while deuteration at phosphorus, affording $[Pt_3(\mu\text{-}PBu^t_2)_2(\mu\text{-H})(PBu^t_2D)(CO)_2]$OTf (**2-D**$_2$) would add the splitting due to $^1J_{PD}$ to the signal at 77.5 ppm; moreover, the corresponding proton-coupled spectrum shows the normal splitting ($^1J_{PH}$ = 360 Hz) of the same signal.

Finally, in the ^{195}Pt{^{1}H} NMR spectrum of **2-D**$_1$, each line of the signal assigned to Pt_3 (−3542.5 ppm) is further split into 1:1:1 triplets, and the value of $^1J_{Pt_3D}$ (136 Hz) is in the expected ratio (6.51 = γ_H/γ_D) with the corresponding value of $^1J_{Pt_3H}$ (888 Hz) found in complex **2**. As expected, and opposite to what is observed in **2**, the signal remains unchanged in the corresponding proton-coupled spectrum.

A similar behavior was observed for the signal assigned to Pt_1 (−4335 ppm), which is also directly bonded to deuterium, but an accurate evaluation of $^1J_{Pt_1D}$ was prevented by some broadening and weakening of the signal.

Following the suggestion of one of the reviewers, we prepared $Pt_3(\mu\text{-}PBu^t_2)_3(D)(CO)_2$ (**1-D**), which was reacted with an equimolar amount of TfOH to give selectively **2-D**$_2$, thus confirming that the H/D position is determined by a kinetic effect rather than by a thermodynamic one, and therefore reinforcing our mechanistic conclusions. Complex **2-D**$_2$ was identified by its NMR spectra, which differ as expected from the corresponding spectra of complexes **2** and **2-D**$_1$ [the ^{2}H NMR (CH_2Cl_2, 293 K) spectrum exhibits only one signal at 6.04 ppm for the P−*D* nucleus (d, $^1J_{PD}$ = 56 Hz, 6.5 times smaller than $^1J_{PH}$ in **2**); the selective presence of a proton in the bridging position is also shown by the proton-coupled ^{195}Pt NMR spectrum, which is identical to the corresponding spectrum of complex **2**].

Characterization of a Kinetic Intermediate. When equimolar amounts of a CD_2Cl_2 solution of complex **1** and TfOH were mixed at −40 °C in a NMR tube, the immediate, quantitative conversion of **1** into a unique kinetic intermediate (**3**) was observed. The resonances of complex **3** disappeared rapidly when the tube was warmed to 20 °C, with the parallel growth of those assigned to **2**, which are then stable for weeks. The ^{31}P{^{1}H} NMR resonances of the three P nuclei in **3** are nearly overlapped at ca. 186.1 (2 P) and 176.0 (1 P) ppm; therefore, the spectrum is very far from first order, with a complex pattern of ^{195}Pt satellites. It is worth noting that one of the signals is considerably shifted compared to that of **1**, which exhibited two

(8) Johnstone, D. H.; Shriver, D. F. *Inorg. Chem.* **1993**, *32*, 1045.

(9) (a) By analogy with this result, we suggest that the hydride signal for the related complex $[Pt_3(\mu\text{-H})(\mu\text{-}PPh_2)_2(PPh_3)_3]X$,[6] carefully but unsuccessfully searched at high fields, could be downfield-shifted, and obscured in the crowded aromatic region. Other downfield-shifted δ_H values have been observed, for example, for Zr,[9b] Mo,[9c] Cu,[9d] and Pt[9e−g] transition-metal hydrides or for Zn,[9h] Hg,[9i] and Sn[9m] hydrides. (b) Manriquez, J. M.; McAlister, D. R.; Sanner, R. D.; Bercaw, J. E. *J. Am. Chem. Soc.* **1978**, *100*, 2716. (c) Miller, R. L.; Lawler, K. A.; Bennett, J. L.; Wolczanski, P. T. *Inorg. Chem.* **1996**, *35*, 3242. (d) Goeden, G. V.; Caulton, K. G. *J. Am. Chem. Soc.* **1981**, *103*, 7354. (e) Lloyd, B. R.; Puddephatt, R. J. *J. Am. Chem. Soc.* **1985**, *107*, 7785. (f) Mole, L.; Spencer, J. L.; Litster, S. A.; Redhouse, A. D.; Carr, N.; Orpen, A. G. *J. Chem. Soc., Dalton Trans.* **1996**, 2315. (g) Schwartz, D. J.; Andersen, R. A. *J. Am. Chem. Soc.* **1995**, *117*, 4014. (h) De Koning, A. J.; Boersma, J.; Van der Kerk, G. J. M. *J. Organomet. Chem.* **1980**, *195*, 1. (i) Kaupp, M.; Malkina, O. L. *J. Chem. Phys.* **1998**, *108*, 3648. (m) Dufermont, J.; Maire, J. C. *J. Organomet. Chem.* **1967**, *7*, 415.

signals at 216.9 (2 P) and 95.2 (1 P) ppm. The spectrum clearly indicates that the kinetic site of protonation is not a phosphorus atom. This is confirmed by the corresponding proton-coupled spectrum, which fails to show the large $^1J_{PH}$, typical of a secondary phosphine (high, clearly observable values of $^1J_{PH} > 135$ Hz have been found also when a P−H bond is agostic).[7b]

Alternative basic sites in **1** are the platinum metals or the Pt−H bond, whose protonation would give, respectively, a dihydride or a dihydrogen complex. However, both these hypotheses were excluded by the ^{1}H NMR spectrum of **3**, which shows signals at 1.42−1.55 ppm (three overlapping *tert*-butyls) and at 17 ppm (broad singlet).[10] Moreover, a unique hydridic signal was found at −2.29 ppm (slightly broadened triplet, $^2J_{PH} = 27$ Hz) flanked by Pt satellites ($^1J_{PtH} = 1114$ Hz, terminal hydride), again notably shifted with respect to the hydride signal in complex **1** (−6.60 ppm). The signal remains practically unchanged in a large *T* interval (−90 to +20 °C) or when the protonation is performed with TfOD in place of TfOH; in this case the only significant difference is the disappearance of the signal at 17 ppm. Therefore, the proton added with TfOH does not contribute to the hydride signal at −2.29 ppm and gives the downfield-shifted resonance at 17 ppm, more easily explained by an O-bonded proton[10] than by a Pt-bonded one. In agreement with these results, in the ^{2}H NMR spectrum (CH_2Cl_2, 233 K) of the reaction of **1-D** with *equimolar* amounts of TfOH, we observed only one signal at −2.3 ppm for Pt−*D* [br s, with satellites, $^1J_{DPt} = 170$ Hz (6.5 times smaller than $^1J_{HPt} = 1114$ Hz)]. An *identical* signal was observed when the reaction was performed with TfOD; in this case the spectrum exhibited only a further broad singlet at 17 ppm. This experiment excludes the fact that the large signal of the *tert*-butyl protons hinders a *second* hydride resonance when the reaction is performed with nondeuterated reagents.

Since none of the expected nuclei (Pt, P, hydride) appeared to have been protonated, and considering that the *tert*-butyl substituents make a sort of envelope that hinders the central $Pt_3(\mu\text{-}P)_3$ core, we can speculate whether **3** arises from a less "classical" interaction, namely, a TfOH···H−Pt or a TfOH···OC−Pt hydrogen bond.

Intramolecular[11] or intermolecular[12] E−H···H−M (E = N, O, C) "proton−hydride" or "dihydrogen" bonds have been discovered and characterized, both in solution[11,12] and in the solid state,[13] during the past decade. However, intermolecular interactions of this type generally cause a negligible or very small *upfield* shift of δ_H(hydride), while we observe a large ($\Delta\delta_H = 4.3$ ppm) *downfield* shift. Moreover, in strong contrast with the formation of a TfOH···H−Pt bond, we do not observe any H/D scrambling at the hydride site by performing the reaction with TfOD. "Dihydrogen" bonds are in fact presumed to be in equilibrium with M(H_2) complexes,[11c] thus promoting H/D exchange (eq 1).

$$\text{E-D}\cdot\cdot\text{H-M} \rightleftarrows \text{E}^{-}\left[\begin{array}{c}\text{H}\\ |\\ \text{D}\end{array}\!\!-\text{M}\right]^{+} \rightleftarrows \text{E-H}\cdot\cdot\text{D-M} \quad (1)$$

The selective formation of **2-D**$_1$ as the final product, when **1** is reacted with TfOD, and of **2-D**$_2$, when **1-D** is reacted with TfOH, is also in marked contrast with the formation of an O−H···H−Pt hydrogen bond.

The above-described set of data are more convincingly explained by an interaction of the acid with one of the oxygen atoms of the carbonyls, which in fact protrude out of the *tert*-butyls' envelope more than the hydride ligand. Actually, the kinetic protonation of a bridging carbonyl is well-known in cluster chemistry.[14] In iron or ruthenium clusters it gives downfield-shifted ^{1}H NMR resonances [13.2 ppm in $Fe_4(\mu\text{-}H)(\mu\text{-}COH)(CO)_{12}$,[14a] 16.1 ppm in $Ru_3(\mu\text{-}H)(\mu\text{-}COH)(CO)_{10}$,[14c] and 15.7 ppm in $Fe_3(\mu\text{-}H)(\mu\text{-}COH)(CO)_{10}$[14b]], which compare well with the resonance found at 17 ppm for complex **3**. The interaction of a proton with a terminal carbonyl has been observed rarely, at least in solution, probably due to the minor basicity of the oxygen atom and to the very fast migration of the proton on the metal or other basic sites of the molecule. To the best of our knowledge, a complete proton transfer to a terminal carbonyl has been previously observed only in a mass spectrometer,[15] while the formation of hydrogen bonds of the M−CO···H−E type has numerous examples in the solid state[16a,b] and has been reported once also in solution, although of an unusual solvent (liquid Xe).[16c,d] The latter study has estimated the enthalpy (−4.6 kcal/mol) of the M−CO···HO

(10) (a) This resonance cannot be assigned to the hydrogen-bonded $TfO^-\cdots$HOTf species, which exhibits a similar downfield-shifted δ_H value (17.15 ppm, CD_2Cl_2, −80 °C),[10b] since **3** is *quantitatively* formed by mixing *equimolar* amounts of **1** and TfOH. (b) Bullock, R. M.; Song, J.-S.; Szalda, D. J. *Organometallics* **1996**, *15*, 2504.

(11) (a) Lee, J. C.; Rheingold, A. L.; Muller, B.; Pregosin, P. S.; Crabtree, R. H. *J. Chem. Soc., Chem. Commun.* **1994**, 1021. (b) Peris, E.; Lee, J. C.; Rambo, J. R.; Eisenstein, O.; Crabtree, R. H. *J. Am. Chem. Soc.* **1995**, *117*, 3485. (c) Xu, W.; Lough, A. J.; Morris, R. H. *Inorg. Chem.* **1996**, *35*, 1549. (d) Park, S.; Ramachandran, R.; Lough, A. J.; Morris, R. H. *J. Chem. Soc., Chem. Commun.* **1994**, 2201. (e) Xu, W.; Lough, A. J.; Morris, R. H. *Can. J. Chem.* **1997**, *75*, 475. (f) Stevens, R. C.; Bau, R.; Milstein, D.; Blum, O.; Koetzle, T. F. *J. Chem. Soc., Dalton Trans.* **1990**, 1429. (g) Van Der Sluys, L. S.; Eckert, J.; Eisenstein, O.; Hall, J. H.; Huffman, J. C.; Jackson, S. A.; Koetzle, T. F.; Kubas, G. J.; Vergamini, P. J.; Caulton, K. G. *J. Am. Chem. Soc.* **1990**, *112*, 4831. (h) Liu, Q.; Hoffmann, R. *J. Am. Chem. Soc.* **1995**, *117*, 10108. (i) Abramov, Y. A.; Brammer, L.; Klooster, W. T.; Bullock, R. M. *Inorg. Chem.* **1998**, *37*, 6317. (l) Chu, H. S.; Lau, C. P.; Wong, K. Y.; Wong, W. T. *Organometallics* **1998**, *17*, 2768. (m) Buil, M. L.; Esteruelas, M. A.; Oñate, E.; Ruiz, N. *Organometallics* **1998**, *17*, 3346. (n) Aime, S.; Férriz, M.; Gobetto, R.; Valls, E. *Organometallics* **1999**, *18*, 2030. (o) Ayllon, J. A.; Sayers, S. F.; Sabo-Etienne, S.; Donnadieu, B.; Chaudret, B. *Organometallics* **1999**, *18*, 3981.

(12) (a) Abdur-Rashid, K.; Gusev, D. G.; Lough, A. J.; Morris, R. H. *Organometallics* **2000**, *19*, 834. (b) Aime, S.; Férriz, M.; Gobetto, R.; Valls, E. *Organometallics* **2000**, *19*, 707. (c) Gründemann, S.; Ulrich, S.; Limbach, H.-H.; Golubev, N. S.; Denisov, G. S.; Epstein, L. M.; Sabo-Etienne, S.; Chaudret, B. *Inorg. Chem.* **1999**, *38*, 2550. (d) Alkorta, I.; Rozas, I.; Elguero, J. *Chem. Soc. Rev.* **1998**, *27*, 163. (e) Ayllon, J. A.; Gervaux, C.; Sabo-Etienne, S.; Chaudret, B. *Organometallics* **1997**, *16*, 2000. (f) Shubina, E. S.; Belkova, N. V.; Epstein, L. M. *J. Organomet. Chem.* **1997**, *536*−*537*, 17. (g) Shubina, E. S.; Belkova, N. V.; Krylov, A. N.; Vorontsov, E. V.; Epstein, L. M.; Gusev, D. G.; Niedermann, M.; Berke, H. *J. Am. Chem. Soc.* **1996**, *118*, 1105. (h) Crabtree, R. H.; Siegbahn, P. E. M.; Eisenstein, O.; Rheingold, A. L.; Koetzle, T. F. *Acc. Chem. Res.* **1996**, *29*, 348. (i) Patel, B. P.; Yao, W.; Yap, G. P. A.; Rheingold, A. L.; Crabtree, R. H. *J. Chem. Soc., Chem. Commun.* **1996**, 991. (m) Peris, E.; Wessel, J.; Patel, B. P.; Crabtree, R. H. *J. Chem. Soc., Chem. Commun.* **1995**, 2175. (n) Wessel, J.; Lee, J. C.; Peris, E.; Yap, G. P. A.; Fortin, J. B.; Ricci, J. S.; Sini, G.; Albinati, A.; Koetzle, T. F.; Eisenstein, O.; Rheingold, A. L.; Crabtree, R. H. *Angew. Chem., Int. Ed. Engl.* **1995**, *34*, 2507.

(13) Braga, D.; De Leonardis, P.; Grepioni, F.; Tedesco, E.; Calhorda, M. J. *Inorg. Chem.* **1998**, *37*, 3337 and references therein.

(14) (a) Aime, S.; Dastrú, W.; Gobetto, R.; Viale, A. *Organometallics* **1998**, *17*, 3182. (b) Pribich, D. C.; Rosenberg, E. *Organometallics* **1988**, *7*, 1741. (c) Neringer, L. R.; Keister, J. B.; Maher, J. *Organometallics* **1990**, *9*, 1900. (d) Chen, C. K.; Cheng, C. H. *Inorg. Chem.* **1983**, *22*, 3378. (e) Whitmire, K. H.; Shriver, D. F. *J. Am. Chem. Soc.* **1981**, *103*, 6754. (f) Fachinetti, G. *J. Chem. Soc., Chem. Commun.* **1979**, 397.

(15) Hop, C. E. C. A.; McMahon, T. B. *Inorg. Chem.* **1991**, *30*, 2828.

(16) (a) Camiolo, S.; Coles, S. J.; Gale, P. A.; Hursthouse, M. B.; Mayer, T. A.; Paver, M. A. *Chem. Commun.* **2000**, 275. (b) Braga, D.; Grepioni, F. *Acc. Chem. Res.* **1997**, *30*, 81 and references therein. (c) Hamley, P. A.; Kazarian, S. G.; Poliakoff, M. *Organometallics* **1994**, *13*, 1767. (d) Lokshin, B. V.; Kazarian, S. G.; Ginzburg, A. G. *J. Mol. Struct.* **1988**, *174*, 29.

Chart 2

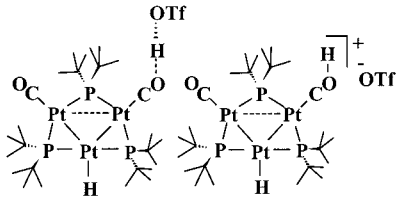

interaction between $Cp^*Re(CO)_2(N_2)$ and perfluoro-*tert*-butyl alcohol (PFTB), and has shown that a hydrogen bond forms even between PFTB and the carbonyls of $Cp^*Re(CO)_2H_2$ or $Cp^*Mn(CO)_2(\eta^2\text{-}H_2)$. On the other hand, the heats of the M−H···H−E interactions are of the same order of magnitude (3−7 kcal/mol),[12h] and Epstein, Berke, and co-workers have shown[12f] that the bulkiness of the phosphine ligands has a strong influence on the hydrogen bond type formed between PFTB and the rhenium complexes $ReH_2(CO)(NO)(PR_3)_2$ [the bulkier phosphines (R = Pr^i) favor the oxygen site (ON−Re in this case) over the Re−H site, preferred when R = Me].

The available experimental data collected on intermediate **3** strongly indicate that it arises from the interaction with TfOH of one of the terminal carbonyls contained in **1**. The relatively high kinetic inertness of **3**, which allowed its observation and partial characterization, is attributed to the particularly high steric encumbrance around all the other basic sites of the molecule, which slows the migration of the proton toward the metal.

Determination of the type of interaction (hydrogen bond or complete proton transfer) between TfOH and CO in intermediate **3** is a more difficult task to be addressed. At first sight, a complete proton transfer could seem more probable, since the introduction of a positive charge could better explain the large downfield shift of δ_H of the hydride and of δ_P of one of the phosphorus nuclei. On the other hand, the values of δ_H(hydride) and δ_P for the phosphorus opposing the Pt−H bond can be greatly influenced by the shape of the Pt_3 triangle. This was found to be isosceles in complex **1**, with one long nonbonding OCPt···PtCO [3.6135(6) Å] and two short HPt−Pt [2.7247(6) and 2.7165(6) Å] distances,[7a] and its isomerization to the equilateral form would reasonably produce marked variations of the values of δ_P and δ_H mentioned above. Since the isosceles and equilateral forms are very close in energy, as nicely shown for the related $Pt_3(\mu\text{-}PPh_2)_3(PPh_3)_2(Ph)$ (**4**)[17a] and confirmed by our finding that $Pt_3(\mu\text{-}PBu^t_2)_3(CNBu^t)_2(H)$, strictly related to **1**, crystallizes in the equilateral form [Pt−Pt = 2.9014(8), 2.9145(7), 3.1709(8) Å],[18] also a relatively small perturbation such as the Pt−CO···HO hydrogen bond could induce a skeletal isomerization to the equilateral form in complex **1** and, therefore, a marked variation of the values of δ_P[17b] and δ_H.

Since the experimental data presently in our hands do not precisely define the intrinsic features of the M−CO/HOTf interaction, we undertook a theoretical investigation on the two different models **3A** and **3B** (Chart 2).

Theoretical Analysis

Method. Theoretical calculations were performed within a density-functional (DF) approach, utilizing the "hybrid" B3LYP[19] functional. This corresponds to a mixture of the Hartree−Fock and Becke[20] exchange functionals, complemented by the Lee−Yang−Parr[21] correlation functional. The calculations utilized the GAUSSIAN98[22] set of programs, running on DEC workstations at ICQEM. A triple-ζ-plus-polarization basis set[23] was employed for the Pt, C, O, P, and H atoms, except for the hydrogen atoms in PH_2 groups, for which a 6-31G basis set[24] was utilized. The TZVP basis set for the Pt atom uses pseudopotentials[25] and incorporates spin−orbit averaged relativistic effects.

To give a more quantitative idea of the strength of selected bonds involved in the various model compounds, a Bader topological analysis[26] (not supported by GAUSSIAN98) was performed at the crudest possible level by simply locating the critical points of the total electron density along the bond paths.

Modeling. Most of the theoretical simulations considered systems in the gas phase, but attempts were made to selectively introduce solvent effects. The calculations were performed on simplified models of **1**, **3A**, and **3B** (for the sake of simplicity, in the following we will not distinguish among **1**, **3A**, and **3B** and their model analogues). A detailed description of the large PBu^t_2 groups would in fact have made the calculations exceedingly heavy in terms of CPU time. They were therefore replaced by PH_2 groups; to make the models as realistic as possible, the hydrogen atoms were placed along the P−C bond axes, at a P−H distance chosen to reproduce as closely as possible the one-electron energies of the two phosphorus lone pairs of the phosphido ligand in the gas phase, i.e., the orbitals directly involved in the Pt−P interaction (a similar "pseudoatom" procedure has been adopted previously).[27] A complete geometry optimization of such model compounds would then be meaningless, since one can expect that only the electronic structure of the corresponding molecules will be reasonably reproduced, but not the steric factors which are essential for geometry predictions. The main $Pt_3(\mu\text{-}P_3)$ skeleton of **1**, **3A**, and **3B** was therefore frozen to the experimentally derived geometry of **1**.[7a] The only available degrees of freedom were associated with the hydrogen involved in the protonation or complexation process, and with the Pt−H hydride and the two CO groups. The triflic residue was allowed to fully relax its structure.

Results. The values of selected optimized geometrical parameters for triflic acid, for the triflic anion, and for **1**, **3A**, and **3B** are given in Table 1, together with the values of the

(17) (a) Bender, R.; Braunstein, P.; Dedieu, A.; Ellis, P. D.; Huggins, B.; Harvey, P. D.; Sappa, E.; Tiripicchio, A. *Inorg. Chem.* **1996**, *35*, 1223. (b) A remarkable deshielding (23 ppm) has been observed for δ_P of one of the μ-P nuclei on going from the isosceles to the equilateral isomeric form of complex **4**.[17a]

(18) Leoni, P.; Marchetti, F.; Pasquali, M.; Quaglierini, S.; Sbrana, F.; Albinati, A. Manuscript in preparation.

(19) Becke, A. D. *J. Chem. Phys.* **1993**, *98*, 5648.

(20) Becke, A. D. *Phys. Rev. B* **1988**, *38*, 3098.

(21) Lee, C.; Yang, W.; Parr, R. G. *Phys. Rev. B* **1988**, *37*, 785.

(22) Frisch, M. J.; Trucks, G. W.; Schlegel, H. B.; Scuseria, G. E.; Robb, M. A.; Cheeseman, J. R.; Zakrzewski, V. G.; Montgomery, J. A., Jr.; Stratmann, R. E.; Burant, J. C.; Dapprich, S.; Millam, J. M.; Daniels, A. D.; Kudin, K. N.; Strain, M. C.; Farkas, O.; Tomasi, J.; Barone, V.; Cossi, M.; Cammi, R.; Mennucci, B.; Pomelli, C.; Adamo, C.; Clifford, S.; Ochterski, J.; Petersson, G. A.; Ayala, P. Y.; Cui, Q.; Morokuma, K.; Malick, D. K.; Rabuck, A. D.; Raghavachari, K.; Foresman, J. B.; Cioslowski, J.; Ortiz, J. V.; Stefanov, B. B.; Liu, G.; Liashenko, A.; Piskorz, P.; Komaromi, I.; Gomperts, R.; Martin, R. L.; Fox, D. J.; Keith, T.; Al-Laham, M. A.; Peng, C. Y.; Nanayakkara, A.; Gonzalez, C.; Challacombe, M.; Gill, P. M. W.; Johnson, B. G.; Chen, W.; Wong, M. W.; Andres, J. L.; Head-Gordon, M.; Replogle, E. S.; Pople, J. A. *Gaussian 98*, revision A.6; Gaussian, Inc.: Pittsburgh, PA, 1998.

(23) Schafer, A.; Huber, C.; Ahlrichs, R. *J. Chem. Phys.* **1994**, *100*, 5829.

(24) Hehre, W. J.; Ditchfield, R.; Pople, J. A. *J. Chem. Phys.* **1972**, *56*, 2257.

(25) Andrae, D.; Haeussermann, U.; Dolg, M.; Stoll, H.; Preuss, H. *Theor. Chim. Acta* **1990**, *77*, 123.

(26) Bader, R. F. W. *Atoms in Molecules: A Quantum Theory*; Oxford University Press: Oxford, 1990.

(27) Fortunelli, A.; De salvo, A.; Salvetti, O.; Albertazzi, E. Cluster Models for Surface and Bulk Phenomena. In *NATO-ARW Proceedings*; Pacchioni, G., et al., Eds.; Plenum Press: New York, 1992.

Table 1. Optimized Values of Total Energies (E), Electrostatic Solvation Free Enthalpies in CH_2Cl_2 at 298 K [$\Delta G_s°$(el)], and Selected Geometrical Parameters for the Compounds Considered in the Present Work[a]

	TfO^-	TfOH	**1**	**3A**	**3B**
E	−961.767724	−962.256324	−1613.415400	−2575.678352	−2575.448762
$\Delta G_s°$(el)	−44.6	−4.3	−1.6	−2.5	−36.8
S−O	1.477	1.627		1.613	
SO−H		0.9715		0.9788	
H−OC				1.914	0.9817
O−C			1.151	1.152	1.253
C−Pt			1.913	1.897	1.835
Pt−H			1.598	1.599	1.589
α(H−O−C)				148.0	115.9
α(O−C−Pt)			179.1	179.8	151.0

[a] Total energies in atomic units (1 au = 627.51 kcal/mol), solvation free enthalpies in kcal/mol, distances in angstroms, and angles in degrees.

Table 2. Values of the Total Electron Density (e/Å^3) at the Critical Points Corresponding to the Various Bonds of **1**, **3A**, and **3B**, As Derived from DF Calculations

molecule	Pt−C	C−O	O−H
1	0.121	0.476	
3A	0.128	0.466	0.0232
3B	0.143	0.398	0.333

optimized total energies. For all models stable local minima were located on the energy surface. In **3B** the acidic hydrogen atom lies on the molecular plane, and is oriented as shown in Chart 2. Alternative stable conformations can be obtained by a 180° rotation around the C−Pt or C−O bonds, but lie higher in energy by 0.86 and 1.6 kcal/mol, respectively. In **3A** one finds a similar configuration with the triflate residue above the plane of the molecule (Chart 2).

The theoretically predicted distances compare reasonably well with the experimental ones for the triflic anion and **1**: for example, the experimental value of R(S−O) is 1.428 Å[28] and that for R(O−C) is 1.166 Å,[7a] whereas R(C−Pt) comes out to be appreciably larger than the experimental value (1.814 Å),[7a] in agreement with previous results.[29] From an analysis of the geometrical parameters reported in Table 1, the following considerations can be drawn.

(a) The S−O distance found in **3A** is intermediate between the corresponding distances in TfOH and TfO^-. The SO−H bond is less affected by the formation of the hydrogen bond.

(b) The increase of the C−O distance and the reduction of the C−Pt distance in **3B** certify a substantial reduction of the CO bond order and the parallel strengthening of the C−Pt interaction. The values of the HOC (115.9°) and OCPt (151.0°) angles are in agreement with such a picture. A further confirmation comes from a Bader analysis[26] of the total electron density for **1**, **3A**, and **3B**: see Table 2 for the values at the critical points corresponding to the C−Pt, O−C, and H−O bonds. These values can be related to the strength of these bonds,[26] and in fact it is found that the C−O bond weakens along the sequence **1**−**3A**−**3B**, whereas the C−Pt bond strengthens, and that the H−O interaction in **3A** is typical of a hydrogen bond. For comparison, the corresponding values (e/Å^3) are 0.483 for free CO, 0.362 for free water, and 0.0252 for the hydrogen bond in the water dimer.

Let us now analyze the theoretical predictions concerning the interaction energies between the different systems.

We start by considering the hydrogen-bonded structure. From Table 1, we see that the dissociation energy of **3A** into **1** plus TfOH is 4.16 kcal/mol ($E_{\mathbf{3A}} - E_{\mathrm{TfOH}} - E_{\mathbf{1}}$). This corresponds to a hydrogen bond of respectable strength: for comparison, the same method and basis set predict a dissociation energy of 5.92 kcal/mol for the water dimer.

One should also keep in mind that the true processes occur in a CH_2Cl_2 solution, so that solvation energies should be taken into account. To this aim, in Table 1 the solvation free enthalpies (CH_2Cl_2, 298 K) of the various molecular species are also reported, as calculated using the polarized continuum model (PCM) method[30] as implemented within the GAUSSIAN98 set of programs. The geometries are those optimized in the gas phase, the theoretical method and basis set are the same as above, and the atomic radii are R(C) = 1.77 Å, R(F) = 1.50 Å, R(S) = 1.98 Å, R(O) = 1.59 Å, R(OH) = 1.59 Å, R(Pt) = 1.72 Å, R(PtH) = 1.72 Å, and R(PH_2) = 2.24 Å (for the TfO^- anion, these values are reduced by a factor of ∼2%). Only the electrostatic component is reported in Table 1, since the values of cavitation and dispersion−repulsion energies are not significant for the model compounds. From an analysis of these results the hydrogen-bonded complex **3A** is stable by ∼0.9 kcal/mol with respect to dissociation into **1** and triflic acid.[31]

It is to be noted that intrinsic errors in these calculations are inherent in both the PCM method, which cannot provide an accuracy better than 1 kcal/mol (at best) for the solvation free enthalpies, and the neglect of zero-point vibrational and rotational corrections. The latter effects, however, are usually rather small, and should not exceed a few tenths of a kilocalorie per mole. Such small energy differencies are anyway particularly difficult to handle with high accuracy using the current theoretical methodologies. To make an example, when, instead of optimizing the structure of **3A** in the gas phase and then evaluating the solvation energy, we performed the optimization by taking simultaneously into account solvation effects, we found that complex **3A** is stable by 1.9 kcal/mol with respect to dissociation. The provisional conclusion is therefore that the kinetic intermediate *might* be associated with a hydrogen-bonded complex.

Let us now consider the full proton-transfer species **3B**. First, we note that the CO groups in **1** are bases of respectable strength, with a first protonation energy [$-(E_{\mathbf{3B}} - E_{TfO^-} - E_{\mathbf{1}})$] of −166.7 kcal/mol. However, **3B** is a stronger acid than triflic acid itself, whose deprotonation energy ($E_{\mathrm{TfOH}} - E_{TfO^-}$) is 306.6 kcal/mol. The latter value is in keeping with the previous theoretical prediction of 303−308 kcal/mol and the experimental

(28) Hagen, K. S.; Armstrong, W. H.; Hope, H. *Inorg. Chem.* **1988**, *27*, 967.
(29) Leoni, P.; Pasquali, M.; Cittadini, V.; Fortunelli, A.; Selmi, M. *Inorg. Chem.* **1999**, *38*, 5257.
(30) Miertus, S.; Scrocco E.; Tomasi. *J. Chem. Phys.* **1981**, *55*, 55.
(31) Since the starting solution is not very diluted (0.04 M), one should consider the possible formation of H-bonded triflic acid dimers. From theoretical calculations the triflic acid is predicted to give dimerization in CH_2Cl_2 solution, with a dissociation energy of ca. 8 kcal/mol. However, this value seems to be largely overestimated, since the experimental data of ref 10b show that triflic acid is not appreciably dimerized at 0.04 M.

estimates of 305.9 ± 2.4 kcal/mol for ΔH and 298.8 ± 2.4 kcal/mol for ΔG.[32] The protonation of **1** by triflic acid is thus expected to have a positive reaction energy of 139.9 kcal/mol ($E_{\mathbf{3B}} - E_{\mathrm{TfOH}} - E_{\mathbf{1}}$). Such a positive ΔE might be overcome in aqueous solution, where the solvation energies of the ions would be scaled by a factor of ~1.5 with respect to those in CH_2Cl_2. CH_2Cl_2 as a solvent, however, is not strong enough to counteract such a large energy penalty: the protonation energy of **1** by triflic acid is in fact predicted to be +64.4 kcal/mol after allowing for the solvation corrections reported in Table 1 (+68.4 kcal/mol if allowing also for the dimerization process).

To give an idea of the kind of accuracy that can be obtained from such an approach, we report that the reaction energy for the proton exchange in water

$$H_2O + H_2O \rightarrow H_3O^+ + OH^-$$

is predicted to be +236.0 kcal/mol in the gas phase, +17.9 kcal/mol in an aqueous solution, and +75.7 kcal/mol in a CH_2Cl_2 solution (electrostatic solvation energies have been utilized, which however do not differ too much from total solvation energies), to be compared with an experimental value of +19.2 kcal/mol for the full ΔG_r in an aqueous solution. The rotovibrational corrections in this case amount to only about −0.3 kcal/mol. It is thus clear that, even though the present approach may not be particularly accurate, it cannot be in error by more than something like 10 kcal/mol, thus excluding the formation of **3B** as a stable intermediate.

We also examined the possibility that the skeleton of **1** is affected by protonation or complexation with triflic acid. In fact, as reminded above, it is known that this type of complex can exhibit isosceles and equilateral geometries very close in energy. Calculations have thus been performed on structure **3B′**, obtained by freezing the $Pt_3(\mu\text{-}PH_2)_3$ skeleton as found in the "equilateral" $Pt_3(\mu\text{-}PBu^t_2)_3(CNBu^t)_2(H)$.[18] However, **3B′** appears to be still less stable than **3B**.

If these results are reasonably accurate, the conclusion is that the kinetic intermediate *cannot* be associated with a complete proton transfer between the triflic acid and **1**, forming separate ions.

A further possibility that must be considered is the formation of a tight ion pair in CH_2Cl_2. The electrostatic interaction energy between the protonated cation and the triflic anion in **3B** might in fact compensate for the loss of solvation energy (the formation of such ionic pairs is quite common in not strongly polar solvents such as CH_2Cl_2).[33]

Calculations have thus been performed in which the energy of an intimate ion pair was optimized in a CH_2Cl_2 solution, i.e., by optimizing the total (internal + electrostatic) solvation energy: the coordinates of the two ions in **3B** were kept as those optimized separately, and the relative disposition of the two ions was left as the only available degree of freedom. The result is that an ion pair was actually found from these calculations, with $R(SO\cdots H) \approx 1.3$ Å, at an energy ~7 kcal/mol higher than that of the hydrogen-bonded complex **3A**. The conclusion is thus that the complex **3A** still remains the most probable candidate to represent the structure of the kinetic intermediate, with a solvated ion pair species reasonably close in energy, which can be available as a first step in the evolution of the intermediate toward the final product **2**.

(32) Otto, A. H.; Steiger, T.; Schrader, S. *J. Mol. Struct.: THEOCHEM* **1998**, *471*, 105.
(33) Bos, M.; Dahmen, E. A. M. F. *Anal. Chim. Acta* **1973**, *63*, 185.

Summary and Conclusions

The high steric hindrance around the Pt_3 core of $Pt_3(\mu\text{-}PBu^t_2)_3(H)(CO)_2$ (**1**) can be reduced by protonation with triflic acid. The reaction was shown to give $[Pt_3(\mu\text{-}PBu^t_2)_2(\mu\text{-}H)(CO)_2(PBu^t_2H)]OTf$ (**2**), in which one of the bulky bridging phosphides has been transformed into a secondary phosphine, and shifted to a more peripheral, terminal position. The reaction carried out with TfOD has clearly demonstrated that the acidic proton is transferred to a metal center, while the secondary phosphine is formed after the coupling of a phosphide and the hydride ligand contained in **1**. Preceding these steps, there is intermediate **3**, stable at low temperatures. Its NMR features indicate that the acidic proton has not yet entered the $Pt_3(\mu\text{-}P)_3$ core, and strongly suggest either a hydrogen-bonding interaction or a complete proton transfer from TfOH to one of the carbonyl ligands.

An ab initio theoretical analysis has shown that the ionic model (**3B**) appears to be reasonable only if stabilized by an electrostatic interaction in a contact ion pair. Both types of interactions lie on stable local minima on the energy surface, and are plausible intermediates with well-defined geometric features. The energy difference between the hydrogen-bonded (**3A**) and proton-transfer (**3B**) models is comparable with the uncertainties of the method, so that, although the former appear to be more stable, we cannot definitely exclude the second.

Experimental Section

General Data. The reactions were carried out under a nitrogen atmosphere, by using standard Schlenk techniques. $Pt_3(\mu\text{-}PBu^t_2)_3(H)(CO)_2$ (**1**) was prepared as previously described;[7a] $Pt_3(\mu\text{-}PBu^t_2)_3(D)(CO)_2$ (**1-D**) was prepared by an analogous procedure, starting from PBu^t_2D in place of PBu^t_2H.

Solvents were dried by conventional methods and distilled under nitrogen prior to use. IR spectra (Nujol mulls, KBr) were recorded on a Perkin-Elmer FT-IR 1725X spectrophotometer. NMR spectra were recorded on a Varian Gemini 200 BB instrument; frequencies are referenced to the residual resonances of the deuterated solvent (^{1}H), 85% H_3PO_4 (^{31}P), and H_2PtCl_6 (^{195}Pt).

Preparation of $[Pt_3(\mu\text{-}PBu^t_2)_2(\mu\text{-}H)(PBu^t_2H)(CO)_2]OTf$ (2). An orange dichloromethane (5 mL) solution of complex **1** (120 mg, 0.111 mmol) turned immediately yellow after the addition of TfOH (20 μL, 0.222 mmol). A sample of the solution was shown (^{31}P NMR) to contain only complex **2**. The volume of the solution was reduced to ca. 2 mL; after the addition of Et_2O (15 mL), complex **2** precipitated out as a yellow powder and was filtered and *vacuum* dried (95 mg, 70% yield); $[Pt_3(\mu\text{-}PBu^t_2)_2(\mu\text{-}D)(PBu^t_2H)(CO)_2]OTf$ (**2-D$_1$**) was prepared similarly (65% yield), by using TfOD in place of TfOH. Anal. Calcd for $C_{27}H_{56}F_3O_5P_3Pt_3S$: C, 26.4; H, 4.60. Found: C, 26.3; H, 4.56. IR (KBr, Nujol): 2050 s, 2026 s (ν_{CO}), 1272 s, 1147 s, 1032 s, 637 m (uncoordinated triflate) cm^{-1}.

When equimolar amounts of **1** and TfOH (or TfOD) were mixed in CD_2Cl_2 at −40 °C in a NMR tube, we observed the immediate quantitative conversion of **1** into intermediate **3**, which is quantitatively converted into complex **2** after a few minutes at 20 °C. Finally, analogous results were obtained when equimolar amounts of complex **1-D** and TfOH (or TfOD) were mixed in CH_2Cl_2 at −40 °C in a NMR tube. See the Results and Discussion for the NMR spectra of **2**, **3**, and their deuterated analogues.

Acknowledgment. Italian Consiglio Nazionale delle Ricerche (CNR) and Ministero dell' Università e della Ricerca Scientifica e Tecnologica (MURST), Programmi di Interesse Nazionale, 2000−2001, are gratefully acknowledged for financial support.

Supporting Information Available: Input files for the in vacuo optimization of the five compounds described in Table 1. This material is available free of charge via the Internet at http://pubs.acs.org.

IC001309M